

**INTRODUCTION:** 15286 is a two-component rock: a piece of regolith breccia is intruded by and/or coated with a vesicular black glass (Fig. 1). Limited data suggest that the glass is fairly similar to but not identical with local soils. The glass composition is a moderately good glass-former, though not equivalent to commercial glass. The breccia is a typical medium gray regolith breccia with glass, mineral, and lithic fragments in a low-porosity matrix. It is coherent to tough. Zap pits occur as few to many on all surfaces, and are especially well developed on the glass. The sample was collected (along with 15159, 15265 to 15269, 15285, and 15287 to 15289) from the crest of an inner bench on the northeast rim of the 12 m crater, downslope 15 m from the LRV. Like several other samples, it was lying very close to 15265-15267 and may have spalled from it. However, it has not been identified in photographs.

**PETROLOGY:** The breccia and glass were described by Wosinski et al. (1973) and by Winzer et al. (1978) and Winzer (1978). According to Wosinski et al. (1973), the glass is vesicular, with clear and devitrified patches, and vesicles are 100 micron to 10 microns in diameter (however, much larger ones up to 5 mm can be seen macroscopically and in thin sections). The glass contains tiny FeNi and (Fe,Ni)S spheres. The dendritic, devitrified phase is scattered throughout the glass. Winzer et al. (1978) noted that a thin vesicular region separates the breccia and the glass, and that the vesicles are deformed. The Fe and FeS droplets are complex. The glass contains one of the highest proportions of fragments among those of Apollo 15 analyzed by the Winzer group, and is the most heterogeneous (other patches are not so heterogeneous; see Fig. 2a). The dendritic phase consists of tiny crystallites of olivine ( $\text{Fo}_{78-76}$ ), with some elongated, larger (80 microns) crystals being more magnesian ( $\text{Fo}_{83-78}$ ). No pyroxene was observed. Analyses of the rind glass show it to be fairly similar to local soil, but the analysis of Uhlmann and Klein (1976) is less aluminous and more iron-rich.

Mehta et al. (1979) investigated the submicroscopic metal particles in the glass coat. Almost all are rounded and consist of the two-phase assemblage metal and FeS. In the metal, Ni constitutes 9.4 to 15.5%. The sulfide is nearly stoichiometric troilite with up to 1.3% Ni. Coarse (larger than 1 micron) patches are similar to fine particles in both chemistry and structure, indicating that both are meteoritic debris; experiments suggest that the metal formed as fine silicate melt. The structure indicates rapid solidification of metal-sulfide liquids, and does not display the cubic-shaped metal found for reduction to  $\text{Fe}^0$  metal.



Fig. 1a



Fig. 1b

Figure 1. Main mass of 15286. (a) S-71-44952, (b) S-71-44951.

The breccia was found by McKay et al. (1974) to be immature ( $I_s/FeO = 9$  to  $15$ ; listed by Korotev, 1984 unpublished, as 13). It consists of anhedral and angular fragments, including pigeonite, augite, and plagioclase, and many are shocked (Wosinski et al., 1973). Winzer (1978) analyzed five clasts (possibly in the glass coat?) with an area scan technique, finding a fairly restricted range of compositions (23.3 to 25.6%  $Al_2O_3$ ) which he suspected was a function of the portion sampled, and not a good indicator of a limited provenance. Inspection of several thin sections indicates a wide variety of clasts, including mare basalts and possibly KREEP basalts. Glasses are dominantly colorless or yellow, but rare orange/red glass is present. Best and Minkin (1972) included 15286 in an analytical study of glasses, but did not specify data from 15286. An average composition of matrix glass was given by Handwerker et al. (1972) and was deemed to be similar to the coat glass (Table 1).

TABLE 15286-1. Analyses of glass

	Coat	Coat	Matrix
SiO <sub>2</sub> %	47.35	46.1	47.6
TiO <sub>2</sub>	1.44	1.6	1.2
Al <sub>2</sub> O <sub>3</sub>	15.86	14.3	13.3
FeO	12.76	14.2	13.6
MgO	10.42	12.5	13.6
CaO	10.78	10.4	9.8
Na <sub>2</sub> O	0.45	0.8	0.7
K <sub>2</sub> O	0.21	0.1	0.3
Cr ppm	3080	---	---
	(1)	(2)	(3)

- (1) Winzer *et al.* (1978); SEM, considerable uncertainties  
 (2) Uhlmann and Klein (1976), Handwerker *et al.* (1977); microprobe  
 (3) Handwerker *et al.* (1977); microprobe

In a series of papers, the Uhlmann group carried out experiments on their glass and matrix glass compositions to investigate their glass-forming properties, cooling rates, and inferred body sizes for the 15286 glasses (Uhlmann and Klein, 1976; Handwerker et al., 1977; Uhlmann and Onorato, 1979; Uhlmann et al., 1979, 1981; Yinnon et al., 1980). They measured the viscosities of molten glass made to their coat and matrix glass compositions (Fig. 3), and measured crystal growth rates as a function of temperature (Fig. 4). For the glass coat, the glass transition temperature was about 650°C, and maximum growth was  $1.1 \times 10^{-2} \text{ cm}^{-1}$  at an undercooling of about 120°C. The liquidus temperature was determined to be  $1210 \pm 10^\circ\text{C}$ . From TTT diagrams, CT curves show it would be necessary to cool 15286 glass coat at  $120^\circ\text{C min}^{-1}$  or faster to produce a glass (Uhlmann and Klein, 1976). Such a rate is consistent with the thickness presently observed (about 1 cm) suggesting that the molten material intruded (or coated) cold rock. Yinnon et al. (1980) used differential thermal analysis and revised the cooling rate using newly determined nucleation barriers and crystallization statistics analysis to determine a

rate of  $1.3^{\circ}\text{C sec}^{-1}$  ( $80^{\circ}\text{C min}^{-1}$ ) for the glass coat. Uhlmann et al. (1981) used the simplified glass formation model of Uhlmann and Onorato (1979) to determine a critical cooling rate of  $6.2^{\circ}\text{C sec}^{-1}$  for the glass coat composition (compared with  $2^{\circ}\text{C sec}^{-1}$  measured). Handwerker et al. (1977) found that the matrix glass (which they treated as forming in a separate event from the glass coat) had a transition temperature of  $644^{\circ}\text{C}$ . Its liquidus temperature is  $1270^{\circ}\text{C} \pm 10$ ; viscosity and crystal growth rates as a function of temperature are shown in Figures 3 and 4 respectively. From CT curves (Fig. 6) this matrix glass must have cooled in the region below the liquidus at  $80^{\circ}\text{C min}^{-1}$ ; from crystallization statistics the cooling rate was determined to be  $42^{\circ}\text{C min}^{-1}$  to form a glass, i.e., the breccia matrix glass is a better glass-former than the coat. Annealing tests indicate that the matrix formed by cooling of molten material, not a shock-induced crystal-to-glass transition. The calculated thickness for the appropriate cooling is about 3 cm, about that observed for the rock; a more sophisticated analysis would still suggest cooling in a small body, or at the edge of a large body. The matrix glass also precludes much reheating by the glass coat, locally to  $825^{\circ}\text{C}$  perhaps. Yinnon et al. (1980) used differential thermal analysis and used newly determined nucleation barriers and crystallization statistics analyses to determine a cooling rate of  $0.11^{\circ}\text{C sec}^{-1}$  for the matrix glass. Uhlmann et al. (1981) determined a critical cooling rate of  $7.4^{\circ}\text{C sec}^{-1}$  for the matrix glass (compared with  $0.3^{\circ}\text{C sec}^{-1}$  measured).

CHEMISTRY: An analysis, mainly for trace elements, of the matrix was made by Korotev (1984, unpublished) (Table 2, Fig. 7). The rare earths and other incompatibles are enriched a little over local soils, and is more like 15265, from which it may well have spalled.

MICROCRATERS: Brownlee et al. (1973, 1975) studied the depth/diameter relationships for craters on a surface glass chip (Figs. 8, 9). They found no strong dependence of  $P/D_p$  on  $D_p$  (Fig. 8). Combined with data from other rocks, the indications are that most of the projectiles had mean densities of 2 to  $4 \text{ gm cm}^{-2}$  (i.e., silicates, not iron), and had velocities of  $20 \pm 5 \text{ km/sec}$ . The size-frequency distribution (Fig. 9) was made by optical examination of the entire surface glass and SEM examination of a  $7 \text{ mm}^2$  chip (,11). The data agree well with that for 15205 but do not show a depletion in the 1 to 20 micron size range. Horz et al. (1975) noted that the distribution was unique in not showing bimodality (i.e., 1 to 20 micron depletion), and suggested the possibility that the surface was pointing out of the ecliptic and sampling a different micrometeorite population.

PROCESSING AND SUBDIVISIONS: Two loose chips in the sample bag were determined to be fragments of 15286 and numbered ,1 and ,2. Both chips are very glassy and heavily cratered. Both were entirely subdivided (Fig. 10), ,1 by sawing to produce a chip of the glass coat. Most allocations were made from daughters of ,1. ,6 produced thin sections ,33 to ,36 and ,11 produced thin section ,41. A daughter of ,2 (,3) produced thin section ,15. A new chip directly from ,0 (,27) produced thin sections ,29 and ,30, which are regolith breccia, unlike the other dominantly vesicular glass sections. Further chipping from ,0 produced the McKay and co-workers (e.g., Korotev) samples of interior breccia.

TABLE 15286-2. Chemical analyses

		.42
Wt %	SiO <sub>2</sub>	
	TiO <sub>2</sub>	
	Al <sub>2</sub> O <sub>3</sub>	
	FeO	12.3
	MgO	
	CaO	9.6
	Na <sub>2</sub> O	0.56
	K <sub>2</sub> O	
	P <sub>2</sub> O <sub>5</sub>	
	(ppm)	Sc
V		
Cr		2440
Mn		
Co		37.9
Ni		199
Rb		
Sr		135
Y		
Zr		490
Nb		
Hf		12.7
Ba		345
Th		5.4
U		1.53
Pb		
La		34.0
Ce		90
Pr		
NEI		52
Sm		15.8
Eu		1.61
Gd		
Tb		3.09
Dy		
Ho		
Er		
Tm		
Yb		11.0
Lu		1.51
Li		
Be		
B		
C		
N		
S		
F		
Cl		
Br		
Cu		
Zn		
(ppb)	I	
	At	
	Ga	
	Ge	
	As	
	Se	
	Mo	
	Tc	
	Ru	
	Rh	
	Pd	
	Ag	
	Cd	
	In	
	Sn	
	Sb	
	Te	
	Cs	380
	Ta	1490
	W	
Re		
Os		
Ir	5.9	
Pt		
Au	2.2	
Hg		
Tl		
Pb		

References and methods:

(1) Korotev (1984, unpublished); INAA

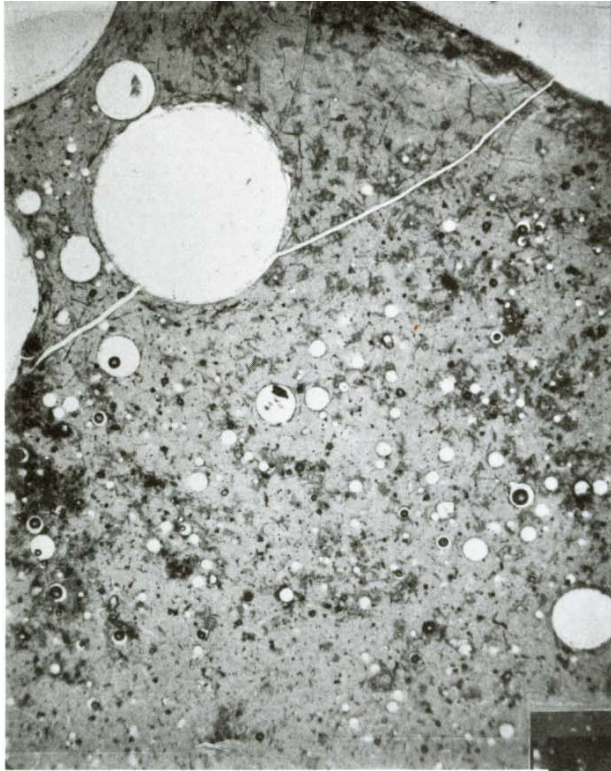


Fig. 2a

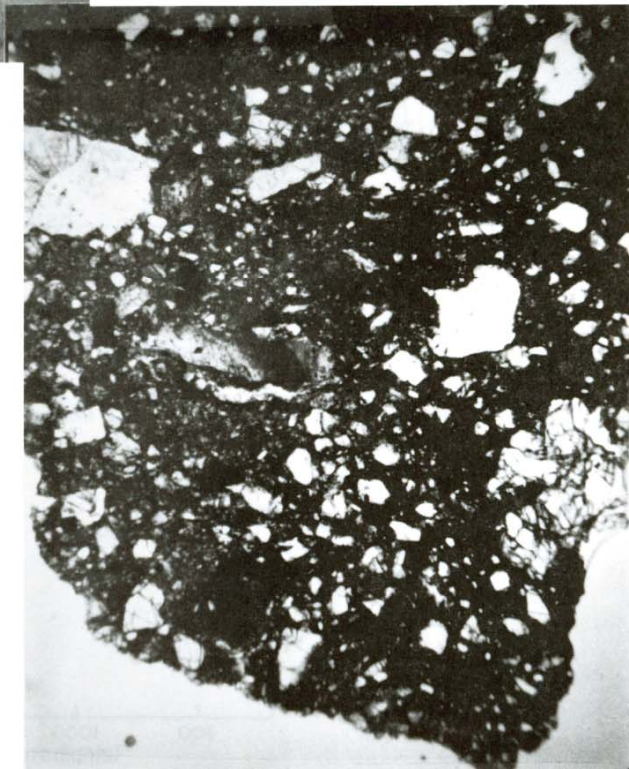


Fig. 2b

Figure 2. Photomicrographs of 15286. Widths about 2 mm.  
Transmitted light. a) 15286,33, vesicular glass coat;  
b) 15286,30, general matrix

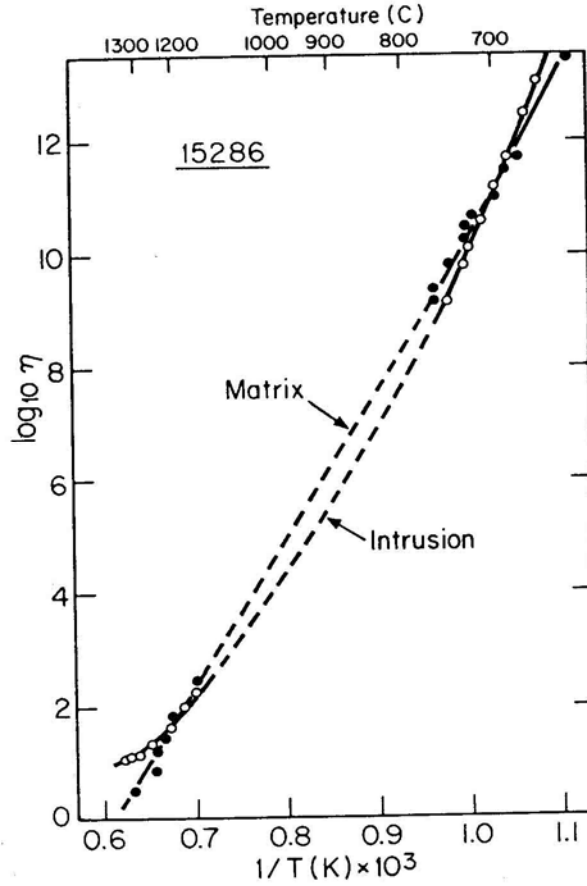


Figure 3. Viscosity vs. temperature for matrix and intrusion (coat) compositions (Handwerker et al., 1977).

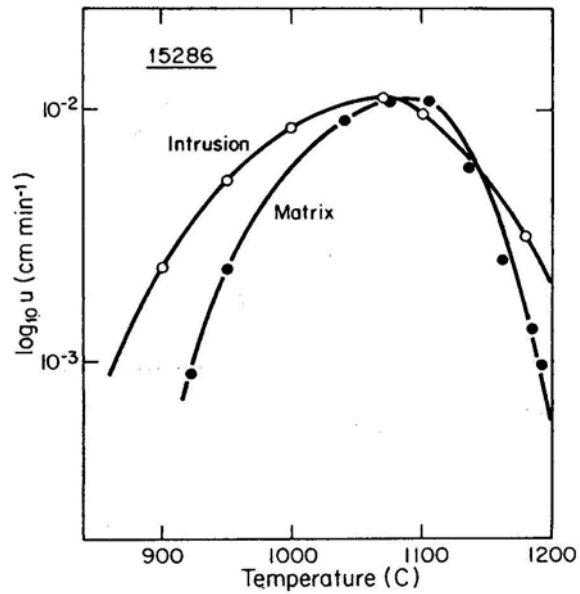


Figure 4. Crystal growth rates vs. temperature for matrix and intrusion (coat) compositions (Handwerker et al., 1977).

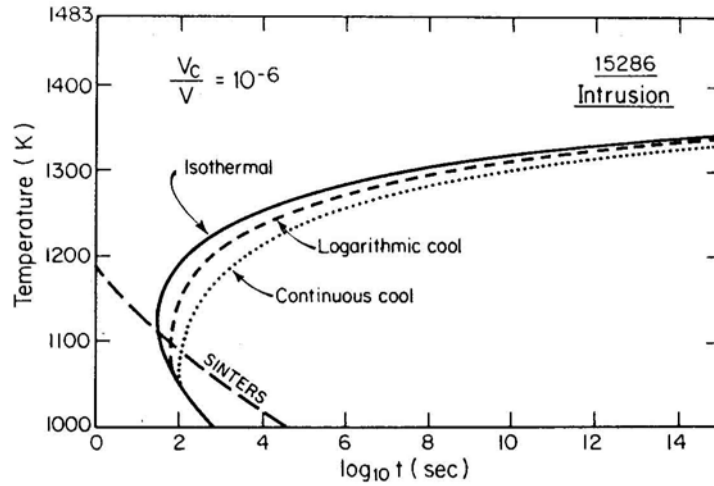


Figure 5. Isothermal time-temperature-transformation, logarithmic cooling (CT), and constant-rate continuous cooling CT curves for glassy intrusion (coat) on 15286 (Handwerker et al., 1977).

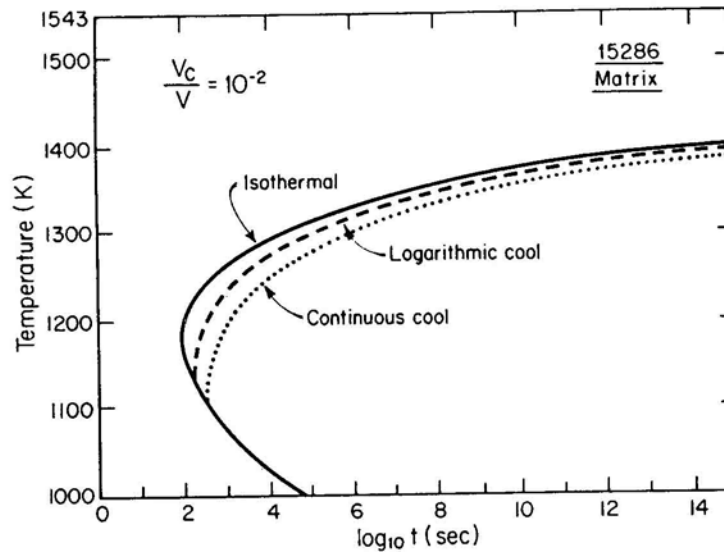


Figure 6. Isothermal time-temperature-transformation, logarithmic cooling (CT), and constant-rate continuous cooling CT curves for the matrix composition of 15286 (Handwerker et al., 1977).

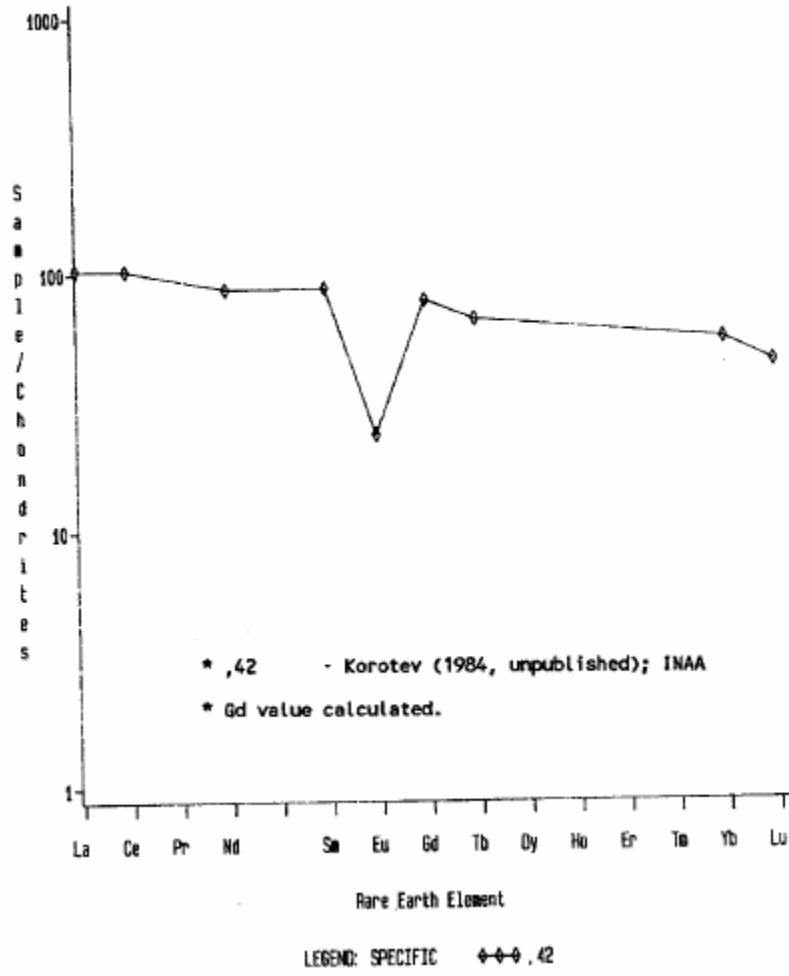


Figure 7. Rare earths in breccia matrix.

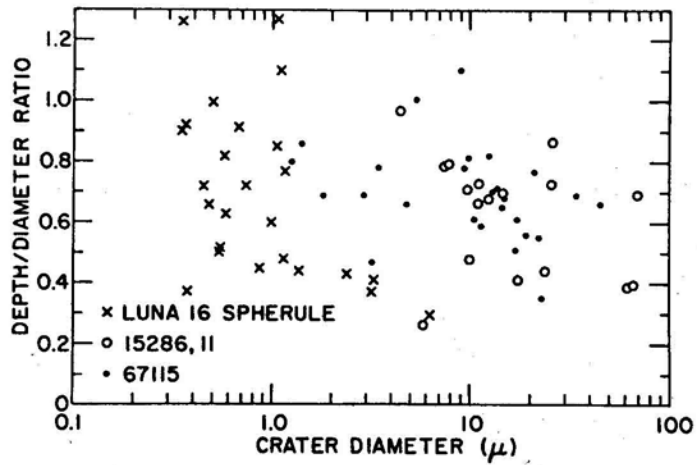


Figure 8. Depth/diameter vs. diameter in glass of 15286 (Brownlee et al., 1973).

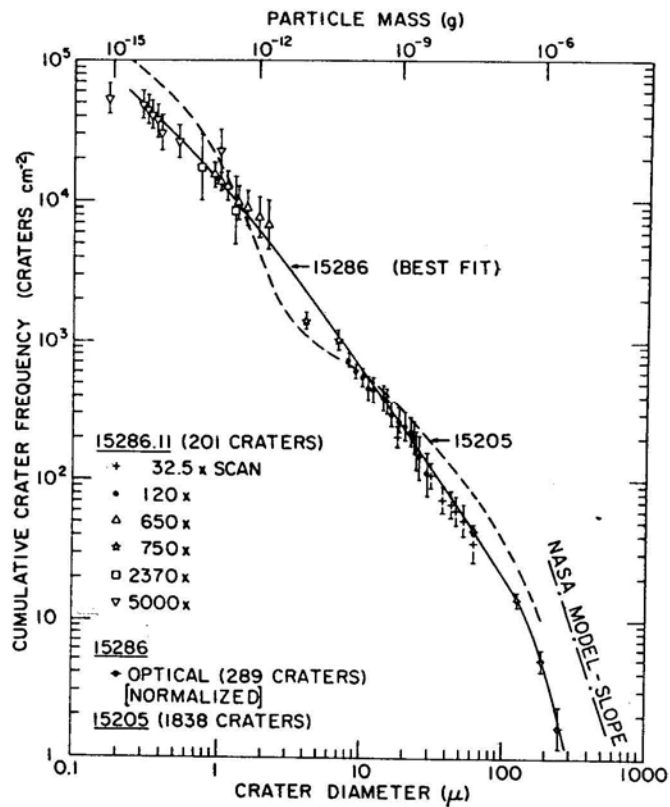


Figure 9. Size frequency for craters on 15286 and 15205. Error bars indicate uncertainty from counting only (Brownlee et al., 1973).

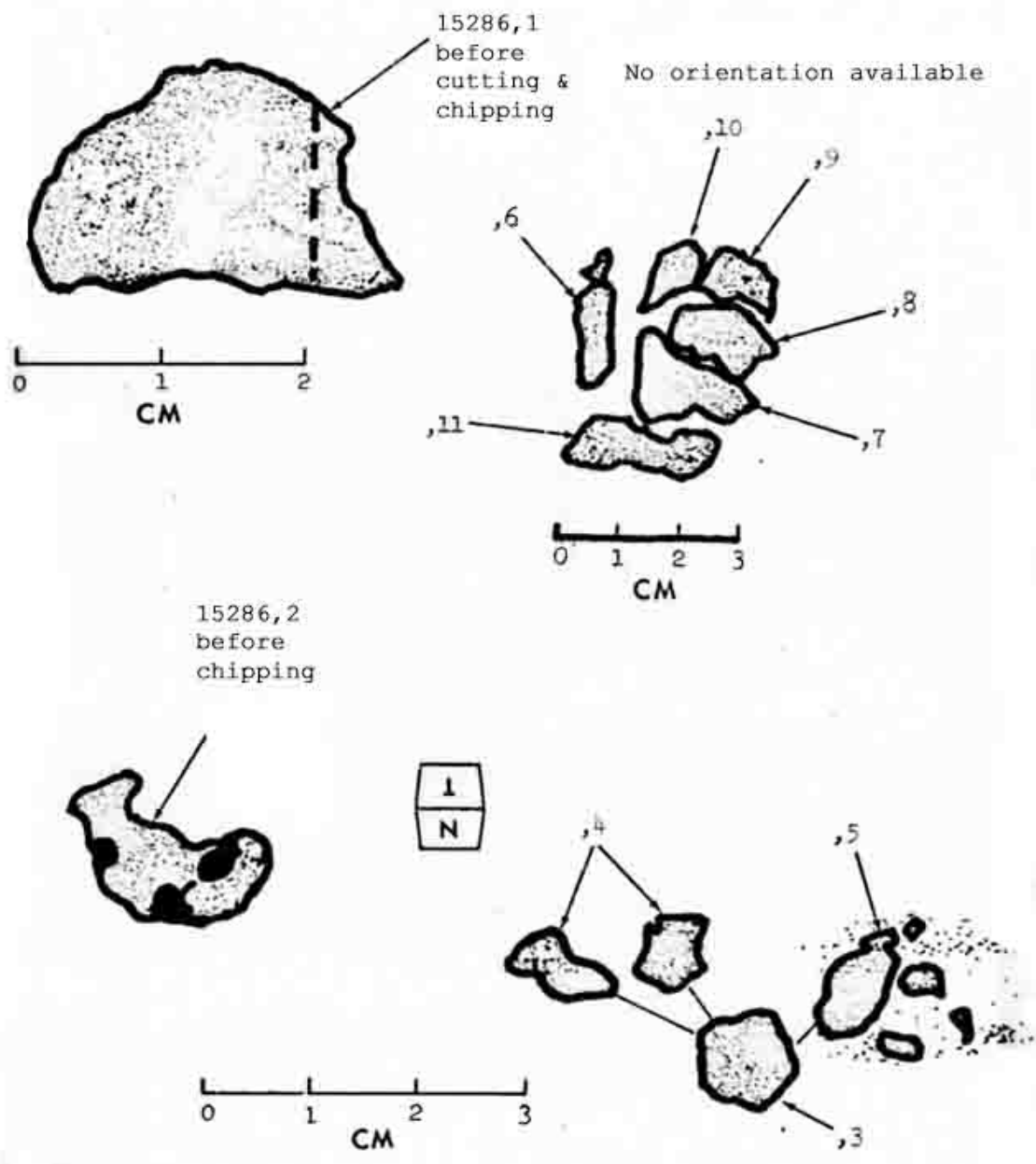


Figure 10. Subdivision of 15286,1 and 15286,2.